

# Evolution of lung pathology in lymphangioliomyomatosis: associations with disease course and treatment response

Suzanne Miller<sup>1,2†</sup>, Iain D Stewart<sup>1†</sup>, Debbie Clements<sup>1,2</sup> , Irshad Soomro<sup>3</sup>, Roya Babaei-Jadidi<sup>1,2</sup> and Simon R Johnson<sup>1,2,4,5\*</sup> 

<sup>1</sup>Division of Respiratory Medicine, NIHR Biomedical Research Centre, London, UK

<sup>2</sup>Nottingham Biodiscovery Institute, University of Nottingham, Nottingham, UK

<sup>3</sup>Department of Pathology, Nottingham University Hospitals NHS Trust, Nottingham, UK

<sup>4</sup>National Centre for Lymphangioliomyomatosis, Nottingham University Hospitals NHS Trust, Nottingham, UK

<sup>5</sup>Nottingham Molecular Pathology Node, University of Nottingham, Nottingham, UK

\*Correspondence: Simon Johnson, Division of Respiratory Medicine, NIHR Biomedical Research Centre and Nottingham Biodiscovery Institute, National Centre for Lymphangioliomyomatosis, University of Nottingham, Nottingham, UK. E-mail: [simon.johnson@nottingham.ac.uk](mailto:simon.johnson@nottingham.ac.uk)

†These authors contributed equally to this work.

## Abstract

Lymphangioliomyomatosis (LAM) is a rare multisystem disease with a variable clinical course. The lungs are infiltrated by nodules of LAM cells, stromal cells and inflammatory cells, causing lung cysts and respiratory failure. We used immunohistochemical markers in lung biopsy and transplant samples from a national cohort of women with LAM with linked clinical data to understand how LAM nodule cell populations changed with disease progression. Marker distribution was examined qualitatively by dual immunohistochemistry, and markers for LAM cells, fibroblasts, lymphatics, mast cells, proliferation, cathepsin K and mTOR pathway activity were quantitated in LAM nodules and compared with clinical features and prospective lung function loss. The LAM cell marker PNL2 was more extensively expressed in those with higher forced expiratory volume in one second (FEV<sub>1</sub>), higher diffusion in the lung for carbon monoxide (DL<sub>CO</sub>) and less extensive disease involvement whilst the converse was true for the protease cathepsin K. Each percentage increase in cathepsin K reactivity was associated with a 0.65% decrease in FEV<sub>1</sub> (95% CI −1.11 to −0.18) and a 0.50% decrease in DL<sub>CO</sub> (95% CI −0.96 to −0.05). Higher reactivity to the mTOR complex 1 activation marker, phospho-ribosomal protein S6, was associated with a better lung function response to rapamycin ( $p = 0.0001$ ). We conclude that LAM nodules evolve with disease progression, with LAM cells becoming outnumbered by fibroblasts. Increasing cathepsin K expression is associated with more severe disease and lung function loss. Markers of mTOR activation predict the response to rapamycin, suggesting that more advanced LAM may be less mTOR responsive and treatments specifically targeted towards LAM associated fibroblasts may have roles as adjuncts to mTOR inhibition.

**Keywords:** lymphangioliomyomatosis; PEComa; PNL2; cathepsin K; disease progression

Received 18 December 2019; Revised 14 February 2020; Accepted 19 February 2020

Conflict of interest statement: Simon Johnson has received grant funding from Pfizer outside the current work.

## Introduction

Lymphangioliomyomatosis (LAM) is a rare, multi-system disease that develops most frequently in premenopausal women and is characterised by progressive lung destruction, dyspnoea and pneumothorax [1]. Mutation and loss of function of the tuberous sclerosis (TSC) genes in the LAM precursor cell leads to activation of the mTOR-signalling node and the clonal expansion of 'LAM cells' expressing smooth muscle

proteins and markers of melanogenesis. In those with early disease, LAM cells are sparse and difficult to detect but, in more established disease, form nodules comprising multiple cell types. LAM nodules contain fibroblasts and lymphatic endothelial cells (LECs) which are recruited or perhaps transdifferentiate under stimulation by lymphangiogenic growth factors, particularly vascular endothelial growth factor-D (VEGF-D) [2]. Inflammatory cells including T-cells and mast cells are recruited, eventually generating a mature

LAM nodule [3–7]. Lung cyst formation is thought to occur by unregulated protease activity, with the cysteine protease cathepsin K (CATK) expressed in LAM nodules and other related tumours, but not normal lung [8–10]. As a result of tissue damage, most women with LAM progressively lose lung function, suffer recurrent pneumothorax and develop respiratory failure [11,12].

Inhibition of mTOR signalling reduces loss of lung function but does not fully arrest lung function decline in all of those treated [13,14]. As the rate of lung function decline and the response to mTOR inhibition vary between patients, it is important to understand which features of the LAM nodule are associated with active disease in order to both target current therapy appropriately and identify new targets for intervention. Whilst a number of studies have identified relationships between nodule and cyst density and disease severity [15–17], it is not known how LAM nodules develop over the course of the disease nor if the individual components of a nodule are related to disease progression and activity.

Here we have examined immunohistochemical markers of LAM cells, fibroblasts, mTOR activation, mast cells, lymphangiogenesis, protease expression and cell proliferation in multiple LAM nodules from closely phenotyped patients, to determine how evolution and variability in nodule biology is associated with clinical features and lung damage.

## Methods

Full details of all methods, including statistical analyses, are provided in the supplementary material.

### Patient cohort, clinical assessment and tissue samples

Women with LAM defined by current ATS/JRS criteria [18] were recruited from the National Centre for LAM in Nottingham UK between 2011 and 2018. The East Midlands Research Ethics Committee approved the study (13/EM/0264) and all participants gave written informed consent. Medical history, CT scanning of the chest and abdomen and full lung function were performed when recruited to the study as part of clinical care. FEV<sub>1</sub> and DL<sub>CO</sub> were performed at each follow-up visit. Prospective change in lung function was calculated by the slope of a regression line of all values of FEV<sub>1</sub> ( $\Delta$ FEV<sub>1</sub>) or DL<sub>CO</sub> ( $\Delta$ DL<sub>CO</sub>) [19]. Treatment response to rapamycin was based

upon the expected values observed in clinical trials and cohort studies of rapamycin in LAM [13,14] and defined as good if either  $\Delta$ FEV<sub>1</sub> or  $\Delta$ DL<sub>CO</sub> was equal to or greater than  $-0.001$  l/year or  $-0.025$  mmol/kPa/min/year respectively and poor below these values. Tissue samples were all taken for clinical care, for diagnosis by the referring centre, after workup at the LAM Centre or from surgical treatment for pneumothorax. All tissues were obtained prior to treatment with rapamycin.

### Histological staining and analysis

Tissue samples were evaluated by a consultant histopathologist (ISo) and a LAM histology score assigned as described [16]. Protein markers were selected to reflect the cell types and proteins within LAM nodules. These comprised smooth muscle actin (SMA), CATK, VEGF-D [8,20,21], fibroblast surface protein (FSP) [5], podoplanin (PDPN) [6] and mast cell tryptase (MCT) [22]. mTOR complex 1 dysregulation was evaluated by anti-phosphorylated ribosomal protein S6 (pS6) and proliferation by proliferating cell nuclear antigen (PCNA). LAM cells were identified using PNL2 [23], other than in dual staining colocalisation studies, where secondary antibody cross reactivity precluded the use of PNL2 and anti-gp100 (the rabbit equivalent of HMB-45) was used. Antibodies are detailed in the supplementary material, Table S1.

After optimisation, immunostaining for each marker was performed in a single batch with markers studied in sequential tissue sections. Whole slide images were captured using a Digital Nanozoomer (Hamamatsu Photonics, UK). Nodules were selected based on their presence in all consecutively stained sections. Regions of interest (ROIs) were selected from areas comprising greater than 70% SMA positive staining and excluding epithelial hyperplasia surrounding nodules from up to five LAM nodules in each tissue. Immunopositivity of ROI images for each marker in sequential sections was quantitated using a validated, semi-automated protocol. The performance of the protocol was visually assessed in 10% of nodules by individuals blinded to the automated result.

### Statistical analysis

Exploratory analyses of marker reactivity were conducted by graphical assessment and hypothesis testing. A Bonferroni adjustment for multiplicity defined a conservative *P* value threshold of  $p = 0.006$ . Coefficient of variation (CV) was used to assess dispersion

of marker reactivity. Relationships between markers were assessed by Pearson correlation. Non-parametric Wilcoxon-Mann-Whitney tests were used to identify associations of tissue average reactivity with clinical phenotypes confirmed by regression analyses in generalised linear models. Sub-analyses at the level of individual nodules were performed in individuals with serial lung function. Quantile regression was used to assess associations of marker reactivity and lung function. Coefficients and robust standard errors were estimated with bootstrapping using 200 replications. Analyses were performed in Stata SE15.1 (StataCorp, TX, USA).

## Results

### Patients and tissue samples

Tissue for histological analysis was obtained from 32 individuals (26 diagnostic biopsies and six explanted lungs at transplantation for severe LAM). Full clinical details were not available for four transplant tissues. The mean age at the time of tissue sampling was 40.8 years with a mean duration of LAM symptoms of 5.9 years. The majority of women had presented with dyspnoea or pneumothorax. Mean FEV<sub>1</sub> at the time of tissue sampling was 67% of predicted and mean prospective loss of FEV<sub>1</sub> following the biopsy was 94 ml/year ( $n = 17$ ). Eleven were treated with rapamycin following tissue sampling for the diagnosis of LAM (Table 1). LAM nodules were identified using SMA staining, regions of interest selected, sequential sections stained for individual markers and quantitated as described (Figure 1A–C).

### Expression of LAM cell and fibroblast proteins

Multiple antigen labelling was used to understand the heterogeneity of LAM nodules and the cellular localisation of the markers used (Figure 1D,E). Examination of tissue from six subjects showed that CATK expression was to some extent co-localised with the LAM cell marker gp100/PMEL (Figure 1D). The lymphatic marker PDPN was located in the endothelial cells lining the lymphatic clefts (Figure 1E) [2] and absent from gp100/PMEL positive LAM cells. SMA was expressed throughout lesions but was excluded from non-cellular areas in some donors (Figure 1F) and from type II alveolar epithelial cells expressing pro-surfactant protein C. The semi-automated quantification protocol gave good agreement with a visual assessment

Table 1. Clinical details of subjects

	Mean (SD) <sup>†</sup> or percentage of cohort*	<i>n</i>
Age (years) <sup>†</sup>	40.8 (9.6)	30
Disease duration (years) <sup>†</sup>	5.3 (5.7)	30
Post-menopause*	31.3	29
First symptom*		
Dyspnoea	28.1	29
Pneumothorax	46.9	29
Angiomyolipoma	9.4	29
None	3.1	29
Ever present*		
Pneumothorax	75.0	28
Lymphatic disease	6.3	28
Angiomyolipoma	46.9	28
Tuberous sclerosis	12.5	28
LAM histology score*		
1	40.6	32
2	40.6	32
3	18.8	32
Lung function <sup>†</sup>		
FEV <sub>1</sub> (% predicted)	67.4 (23.8)	30
DL <sub>CO</sub> (% predicted)	55.4 (23.2)	30
ΔFEV <sub>1</sub> (ml/year)	−94.0 (134.8)	17
ΔDL <sub>CO</sub> (mmol/min/kPa/year)	−0.23 (0.22)	17
ΔFEV <sub>1:rapa</sub> (ml/year)	18.8 (106.7)	11
ΔDL <sub>CO:rapa</sub> (mmol/min/kPa/year)	−0.07 (0.23)	11

Details of 32 biopsies from individuals with LAM. Four transplant samples did not have full clinical data available and not all subjects had sufficient prospective lung function for analysis.

<sup>†</sup>Mean (SD).

\*Percent of cohort with feature present. ΔFEV<sub>1</sub>, regression slope of FEV<sub>1</sub> values; ΔDL<sub>CO</sub>, regression slope of DL<sub>CO</sub> values; Rapa, whilst treated with rapamycin. *n* is the number of subjects for whom data were available.

of nodule staining (see supplementary material, Figure S1).

### Distribution of markers within LAM nodules

One hundred and forty-seven nodules with >70% SMA positivity were selected from 32 subjects (mean 4.6 nodules per sample, range 2–5) resulting in 1319 images for all markers. Differences in the extent of marker reactivity were assessed by coefficient of variation. Mean reactivity for all markers was variable both between individual nodules within tissues and between mean values for whole tissues between individuals (Figure 2 and see supplementary material, Table S2). This variability was present at all disease durations and levels of FEV<sub>1</sub>, DL<sub>CO</sub> and LAM histology score (see supplementary material, Tables S3 and S4). The strongest associations between the expression of different markers were for: cathepsin-K and VEGF-D ( $r = 0.65$ ; d.f.145;  $p < 0.0001$ ), cathepsin-K and PDPN ( $r = 0.56$ ; d.f.142;  $p < 0.0001$ ) and PDPN and VEGF-D ( $r = 0.48$ ; d.f.142;  $p < 0.0001$ ; Figure 2).

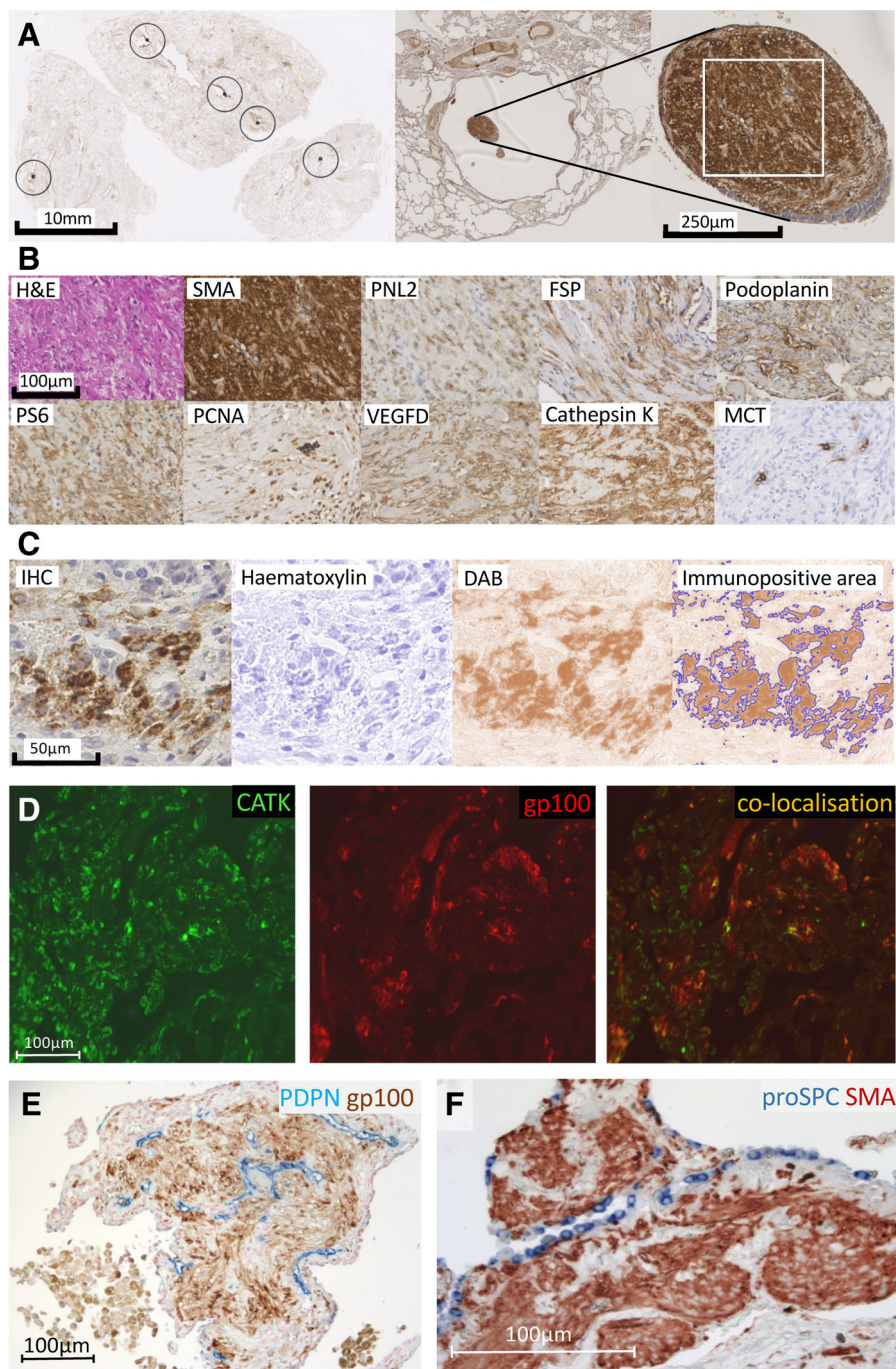


**Figure 1.** Immunohistochemical analysis of LAM nodules and data capture. (A) (Left and central panels) An image of the whole biopsy was captured using a Hamamatsu digital nanozoomer and five LAM nodules identified using SMA staining and morphological criteria. (Right panel) ROI (white square) was selected from the centre of the nodules with the epithelial region excluded. (B) Sequential sections of the ROI were stained with H&E, SMA, PNL2, FSP, podoplanin, phospho-ribosomal pS6, PCNA, VEGF-D, CATK and MCT. (C) ROIs were entered into a semi-automated quantification protocol. Background staining was minimised, a colour deconvolution toolkit was applied to distinguish DAB staining from H&E contrast, and signal thresholds were averaged from five randomly selected ROIs to apply to batch processing of the relevant marker. Noise was minimised and masks were applied to quantify the percentage area of the ROI that was marker positive. Cellular localisation of markers. (D) Co-immunofluorescent staining of CATK with LAM cell (gp100) marker showing CATK in both cell types, but predominantly in fibroblasts. (E) Immunohistochemical detection of glycoprotein-100 (gp100, brown) and PDPN (blue) in a LAM nodule. (F) Anti-pro-surfactant protein C (proSPC, blue) with anti-SMA (red-brown).

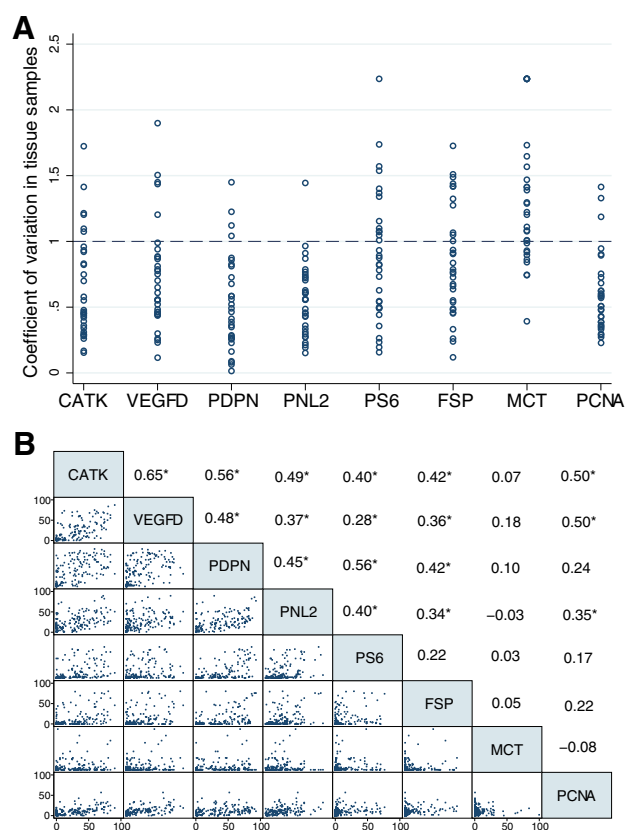


**Figure 2.** Analysis of marker reactivity. (A) Coefficient of variation of nodules within tissue samples presented for each marker. Each circle represents a sample and coefficient of variation is calculated as standard deviation/mean. SMA, PNL2, FSP, PDPN, phospho-ribosomal pS6, PCNA, VEGF-D, CATK and MCT. (B) Matrix of marker reactivity correlations: scatter graphs and *r* values presented. \*Significant following Bonferroni adjustment ( $p < 0.006$ ).

### Association of nodule markers, natural history, lung function and clinical manifestations

How trends of marker reactivity within tissue samples varied with lung function and disease duration were used to assess whether the composition of nodules evolved with disease progression (Figure 3, see supplementary material, Table S5). PNL2 expression was greater in those with higher FEV<sub>1</sub> and DL<sub>CO</sub> whilst CATK was more extensively expressed in those with impaired FEV<sub>1</sub> and DL<sub>CO</sub>. Each percentage decrease in PNL2 reactivity was associated 0.92% decrease percent predicted FEV<sub>1</sub> (%FEV<sub>1</sub>) (95% CI 0.22–1.63) and a 0.87% decrease in %DL<sub>CO</sub> (95% CI 0.19–1.56), whilst each percent increase in cathepsin-K was associated with a 0.65% decrease in %FEV<sub>1</sub> (95% CI -1.11 to -0.18) and a 0.50% decrease in %DL<sub>CO</sub>

(95% CI -0.96 to -0.05). The reciprocal relationship between the expression of LAM cell and fibroblast proteins with disease progression was supported by associations between high PNL2 reactivity, and low CATK reactivity with shorter duration of disease, although this association was not as strong as the relationship with lung function (PNL2 coef. -0.04, 95% CI -0.08 to 0.00; CATK coef. 0.01, 95% CI -0.01 to 0.04; Figure 3).

We next examined the association between nodule protein expression and the clinical manifestations of LAM (see supplementary material, Table S6). pS6 and to a lesser extent PDPN were higher in those with TSC compared with sporadic LAM, although the number of these individuals was small. FSP nodule reactivity was significantly higher in patients with angiomyolipoma 12.4 (IQR 1.2–36.9) compared to those without 1.6 (IQR 0.2–5.2,  $p < 0.001$ ): each percent increment in FSP nodule reactivity was associated with a 6% increase in the likelihood of angiomyolipoma being present (95% CI 1.00–1.12; see supplementary material, Figure S2). Receiver operating characteristic analysis indicated good ability of FSP reactivity within nodules to predict the presence of angiomyolipoma (area under curve 0.72 95% CI 0.63–0.81). A mean sample reactivity threshold of 7.1% for FSP (95% CI 3.5–10.8) provided sensitivity of 0.73 and specificity of 0.85 for the presence of angiomyolipoma (see supplementary material, Figure S2 and Table S6).

### LAM nodule biology is associated with prospective rate of lung function decline and treatment response

We hypothesised that variations in nodule biology would be related to disease activity. There was a linear relationship across nodules for CATK reactivity and rate of loss of DL<sub>CO</sub>: each percentage increment in reactivity being associated with a 0.002 mmol/min/kPa/year loss of DL<sub>CO</sub> (95% CI -0.004 to -0.001. Figure 4, see supplementary material, Table S7). The strength of the association was greatest for those with the most rapid loss of DL<sub>CO</sub>. As pS6 reactivity reflects activation of mTOR complex 1 we examined the relationship between pS6 expression, disease activity and the clinical response to mTOR inhibition. None of the subjects had been treated with an mTOR inhibitor prior to biopsy. Subjects were categorised as having a good or poor response according to lung function slope during treatment, with a good response to treatment defined as a  $\Delta$ FEV<sub>1</sub>  $\geq$  -0.001 l/year or  $\Delta$ DL<sub>CO</sub> of  $\geq$  -0.025 mmol/min/kPa/year and a poor

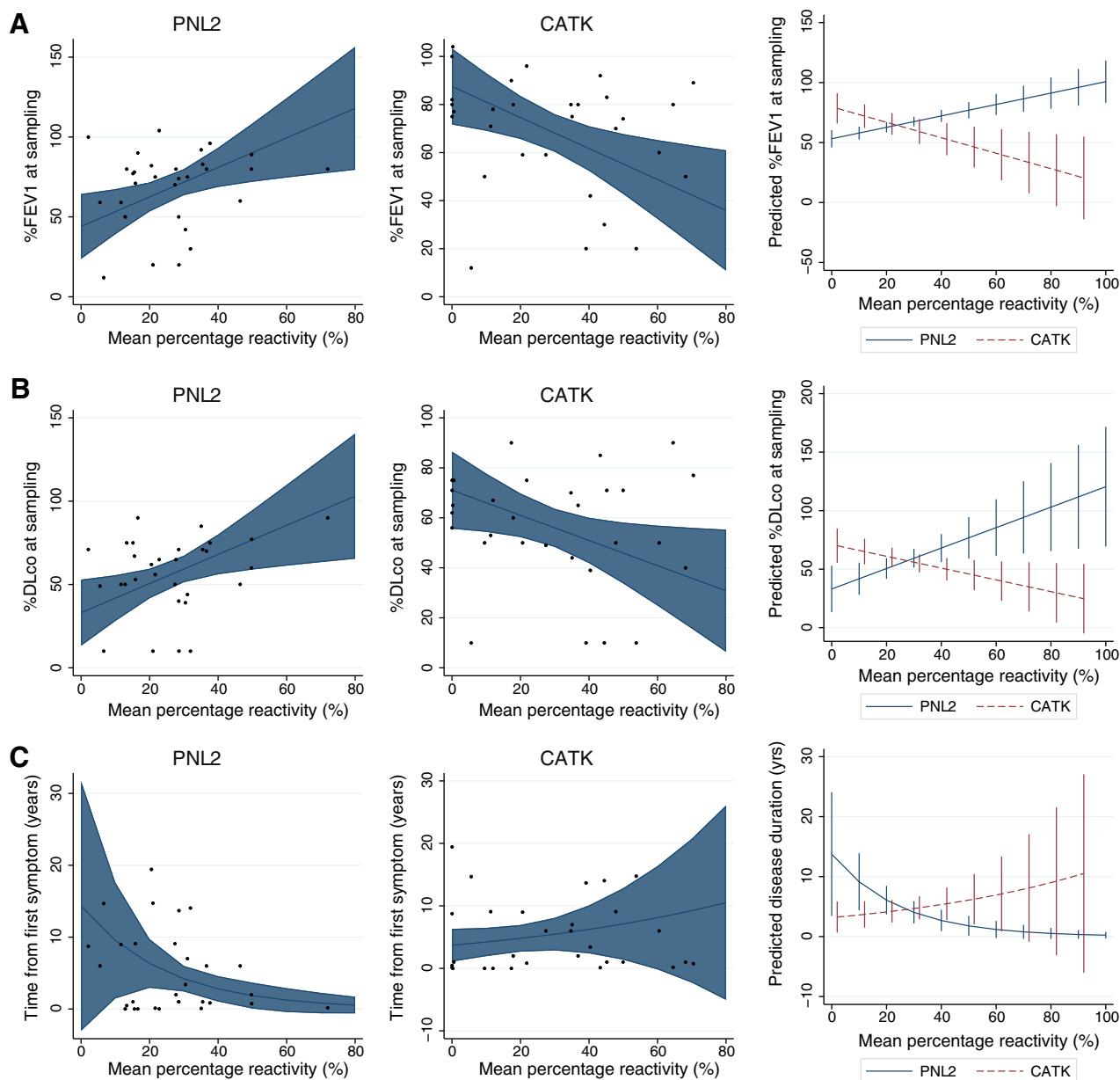


**Figure 3.** Association of LAM nodule reactivity with lung function and disease duration. Mean percentage marker reactivity across tissue samples for PNL2 (left panels) and CATK (central panels). Right panels show regression line fit for both markers. (A) Percent predicted FEV<sub>1</sub> at time of sampling. (B) Percent predicted DL<sub>CO</sub> at time of sampling. (C) Disease duration from first symptom in years.

response less than these values. Six of the 11 treated with rapamycin after biopsy were categorised as having a good response with a mean  $\Delta$ FEV<sub>1</sub>  $0.06 \pm 0.13$  l/year and  $\Delta$ DL<sub>CO</sub> of  $0.04 \pm 0.21$  mmol/min/kPa/year. Poor responders had a mean  $\Delta$ FEV<sub>1</sub> of  $-0.04 \pm 0.02$  and  $\Delta$ DL<sub>CO</sub> of  $-0.26 \pm 0.20$ . pS6 reactivity was higher in nodules from good compared to poor rapamycin responders ( $p = 0.0001$ , Figure 5 and see supplementary material, Table S8).

Regression analysis estimated an 11% increase in likelihood of a good response for each percentage increment in pS6 nodule reactivity (95% CI 1.02–1.21), with similar results following adjustment for time between tissue sampling and start of rapamycin treatment (OR 1.28; 95% CI 1.04–1.58). Based on the lower 95% confidence limit, a pS6 reactivity of 16% or more within a nodule was suggestive of a good response to rapamycin (Figure 4).

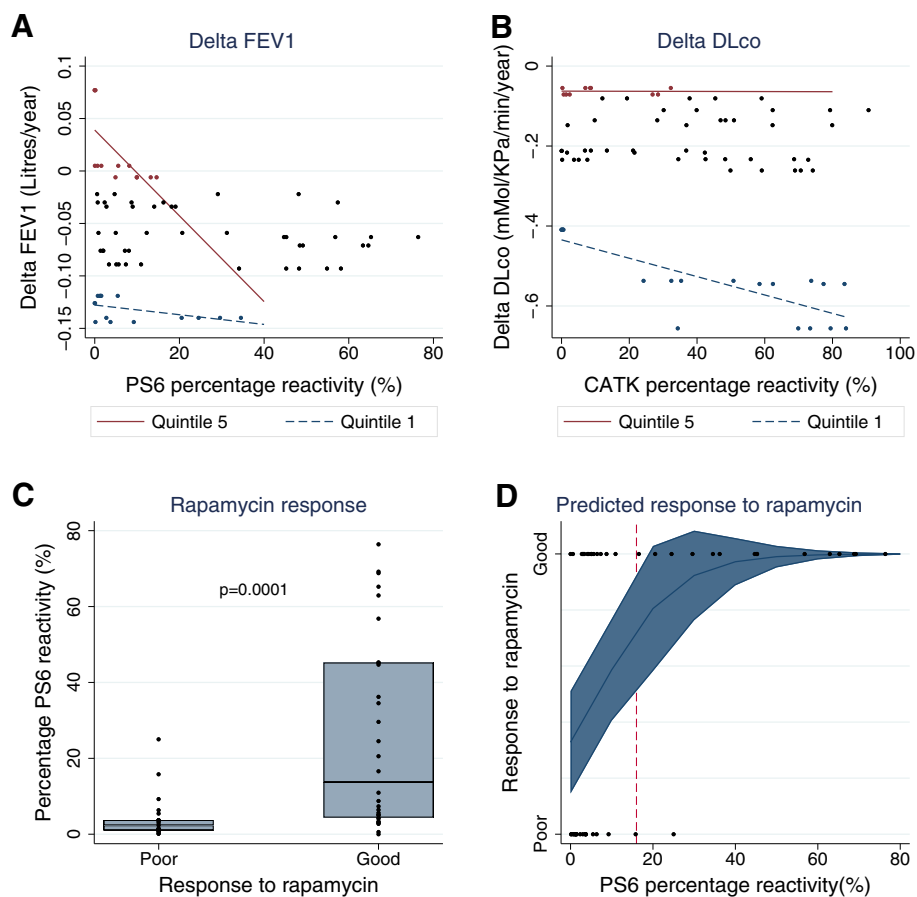


**Figure 4.** LAM nodule reactivity is associated with prospective outcome and treatment response. (A) Phospho-ribosomal pS6 reactivity is plotted against rate of loss of FEV<sub>1</sub> ( $\Delta$ FEV<sub>1</sub>); the regression lines indicate an association in the highest quintile of  $\Delta$ FEV<sub>1</sub> (smallest loss) that is not observed in the lowest quintile (greatest loss). (B) CATK reactivity is plotted against rate of loss of DL<sub>CO</sub> ( $\Delta$ DL<sub>CO</sub>); the regression lines indicate an association in the lowest quintile of  $\Delta$ DL<sub>CO</sub> that is not observed in the highest quintile. (C) Median and interquartile range for pS6 reactivity according to rapamycin response. Wilcoxon–Mann–Whitney  $p = 0.0001$ . (D) Nodule pS6 reactivity according to rapamycin response category with fitted logistic regression line indicated predicted response; the vertical dashed line indicates the percentage pS6 reactivity at which the lower confidence limit of 16% is equidistant between poor and good response categories.

## Discussion

We have shown that the relative expression of protein epitopes within LAM nodules evolves as parenchymal lung disease worsens. As we have been careful to use well validated histological markers of cell types within the LAM nodule: our findings are consistent with LAM cells progressively becoming outnumbered by fibroblasts as disease progresses. The observation that variation in marker reactivity between nodules within individual tissue samples remains across disease severities is consistent with *de novo* nodule formation throughout the course of the disease. A consequence of fibroblast accumulation with disease progression is

the increasing expression of CATK, which is associated with more rapid loss of lung function. We also observe that pS6 expression, a marker of mTOR complex 1 activation, is predictive of the benefit of rapamycin therapy. These findings are important as they suggest that more advanced LAM may be less mTOR responsive and we speculate that treatments targeting LAM associated fibroblasts and CATK could have roles as adjuncts to mTOR inhibition. Furthermore, diagnostic tissue samples may contain prognostic information; predicting future rate of decline and the response to mTOR inhibition.

CATK is a collagen and elastin degrading cysteine protease which is strongly expressed in PEComas and

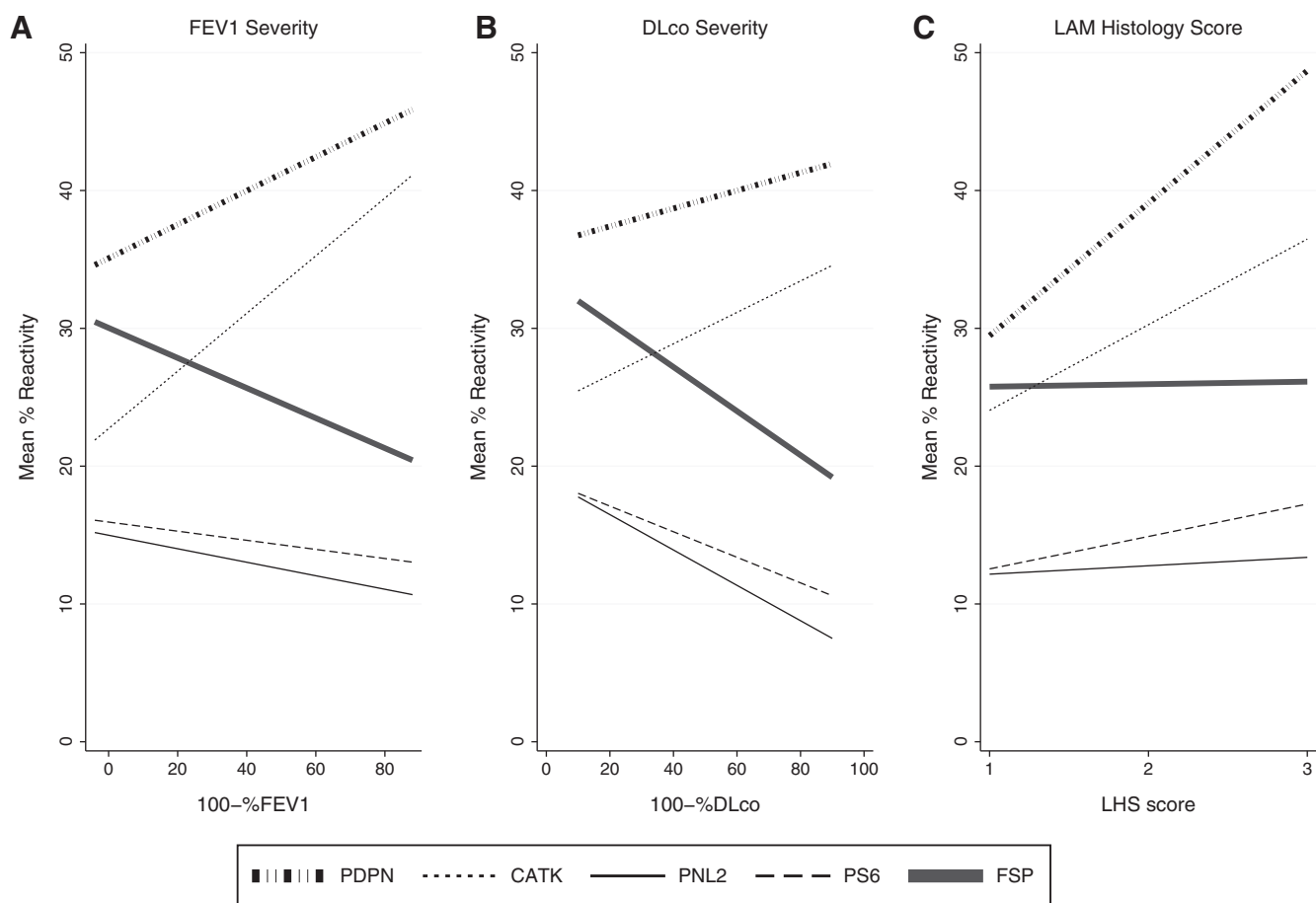


**Figure 5.** Trends in nodule development with disease severity. Linear regression lines fitted between mean reactivity and severity for key markers from the analysis; PDPN, CATK, PNL2, phospho-ribosomal pS6, FSP. (A) Trend of marker reactivity with worsening %FEV<sub>1</sub> (100 – % predicted FEV<sub>1</sub> at biopsy). (B) Trend of marker reactivity with worsening %DL<sub>CO</sub> (100 – % predicted DL<sub>CO</sub> at biopsy). (C) Trend of marker reactivity with increasing LAM histology score (LHS).

LAM [8]. Activation of fibroblast derived CATK in co-cultures of LAM-associated fibroblasts (LAFs) and LAM-derived cells occurs by acidification of the extra-cellular environment in an mTOR-dependent manner [10]. Taken with the current finding that CATK is associated with lung function impairment and future decline in DL<sub>CO</sub>, this suggests that CATK is an important candidate to mediate lung damage in LAM (Figure 5).

More extensive reactivity to PNL2 within nodules is a feature of biopsies from subjects with less extensive disease and better lung function, consistent with a higher proportion of LAM cells within nodules in early disease. As disease progresses, there was a reciprocal relationship between markers associating with LAM cells (PNL2 and pS6) and stromal cells (PDPN and CATK), consistent with a reduction in

LAM cells relative to other cell types (Figure 6). *In vitro*, fibroblasts are attracted to TSC null cells and indeed mutually enhance each other's survival [5]. The increasing proportion of wild-type cells with disease progression is consistent with both the relationship we observed between the expression of pS6 and the lung function response to rapamycin and a clinical study in which those with better preserved lung function at the onset of treatment had the best response to rapamycin [14]. We would suggest that increasing wild-type cells, less dependent upon mTOR signalling, may make more advanced disease less rapamycin sensitive. Further work is required to confirm that pS6 staining in biopsy tissue predicts the response to mTOR inhibition and, moreover, that the response to mTOR inhibitors may be less good in those with more advanced disease where wild type

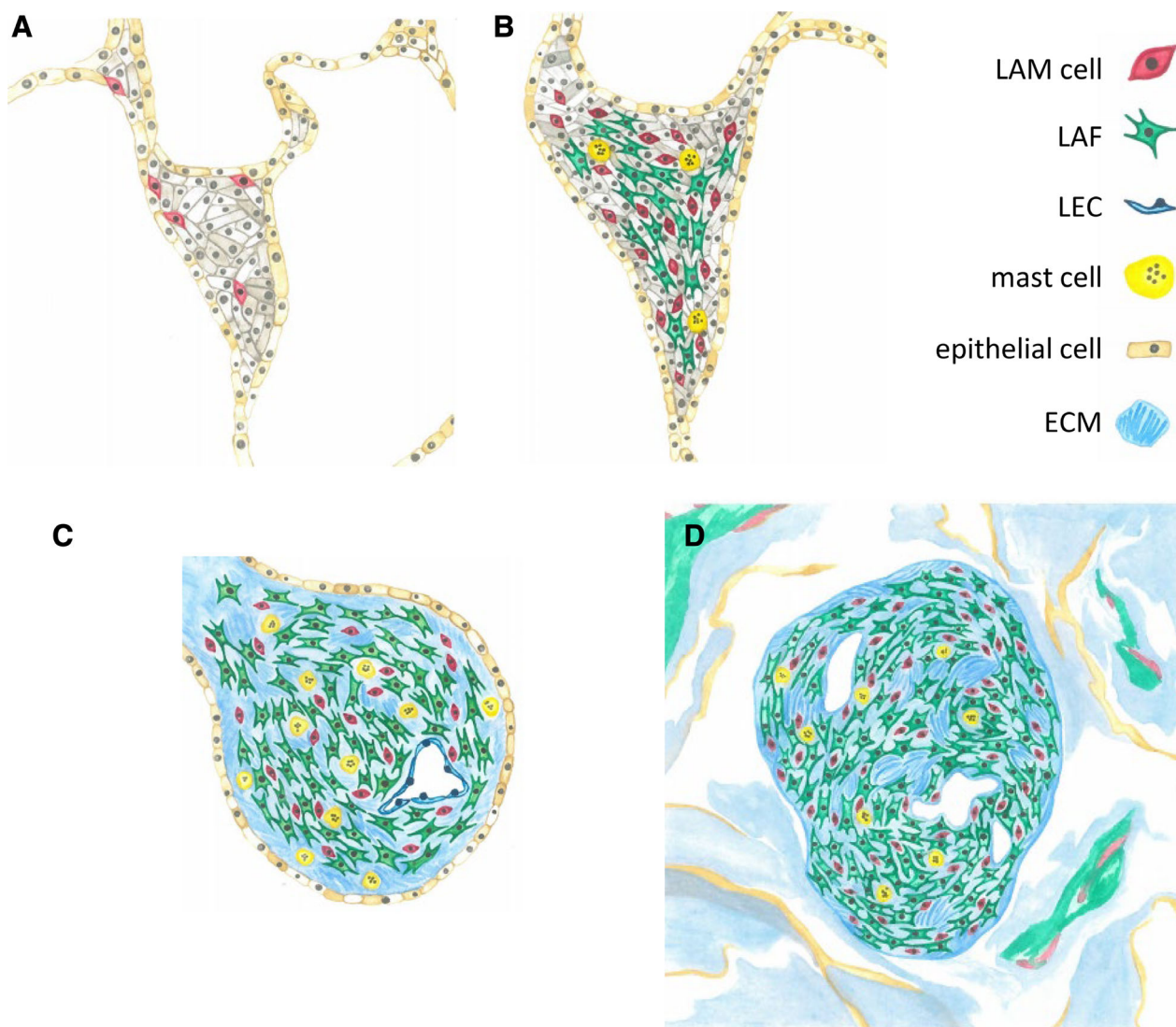


**Figure 6.** Hypothesised development of LAM lesions. (A) LAM cells are initially sparse and isolated in alveolar septae. (B) Over time, LAM cells attract fibroblasts, with the lung parenchyma becoming distorted. (C) LAM cells and LAFs become organised into nodules containing lymphatic clefts lined by PDPN positive LECs, covered by alveolar type II cells and containing inflammatory cells, including mast cells. Discrete nodules line small airways or jut into cystic spaces. Increasingly, LAM cells become outnumbered by LAFs as lung architecture becomes disrupted, which causes FEV<sub>1</sub> and DL<sub>CO</sub> fall. The stromal cells contributing to the LAM nodules are wild type for TSC and therefore reduce the response to mTOR inhibitors. (D) In advanced disease LAFs outnumber LAM cells and are associated with extra-cellular matrix (ECM) deposition. LAM nodules may appear less organised, merging with each other and completely distorting the background lung parenchyma.

stromal cells, with normal mTOR regulation, play a greater role in lung damage.

Based upon antibody target co-localisation from this and our previous work, we observe that cathepsin-K is expressed strongly by LAFs and to a lesser extent by LAM cells [10], VEGF-D is expressed predominantly by LAM cells [6] and PDPN is expressed not only by

lymphatic-related cells but also by LAM associated fibroblasts [24]; analogous to PDPN expression by cancer associated fibroblasts (CAFs) [25,26]. In the current study, the immunostaining pattern shows PDPN is present in lymphatic clefts within nodules but also to some degree in LAFs [2,25]. The expression of PDPN and SMA, which are markers of

fibroblast activation, suggests that LAFs may contribute to tissue damage in LAM, similar to tumour stromal CAFs. Within LAM nodules there are strong correlations between the expression of cathepsin-K, VEGF-D, and PDPN, possibly suggesting the induction of these proteins in different cell types in active disease. This may be due to a direct relationship, such as the lymphangiogenic growth factor VEGF-D inducing PDPN expression through LEC differentiation, or perhaps by a group of linked factors inducing parallel expression of these proteins. The overall expression of the proliferation marker PCNA did not vary over time, although PCNA expression was correlated with cathepsin-K and VEGF-D expression, consistent with these proteins being markers of active disease.

Markers were not strongly associated with disease manifestations with the exception that FSP was highly predictive of the presence of angiomyolipoma. The reason for this association is unclear. However, analogous to metastatic spread in cancer, FSP positive cells may be involved in a pro-metastatic phenotype or in conditioning the renal parenchyma to support angiomyolipoma growth [27]. Further study may offer novel therapeutic strategies for this clinical subset.

There are strengths and weaknesses of our work. Semi-automated analysis of immunohistochemically stained tissue and the application of consistent parameters to quantify marker reactivity allowed the unbiased analysis of a high number of images. However, whilst we have observed robust associations with disease severity, activity and treatment response, initial analyses were exploratory involving multiple associations. Although our original hypotheses were that fibroblasts would accumulate with advancing disease and markers of mTOR activation would predict rapamycin response, other associations were tested mandating statistical corrections to threshold significance values. Although this increased the type II error rate, associations were confirmed in specified generalised linear regression models. As LAM is a very rare disease, and the use of serum markers and comprehensive clinical assessment have reduced the need to obtain lung tissue for diagnosis [18,28], tissue samples with linked prospective outcome data are therefore very scarce which limits the power to detect the association between lung tissue markers and aspects of the LAM phenotype. Mean sample reactivity across tissue was used only where power was sufficient and in sub analyses we were still able to impose conservative confidence intervals generated through adjustment for clustering of nodules within tissue samples, as well as application of bootstrapping to improve error precision. Immunohistochemical labelling is dependent upon antibody

specificity. To improve the association of the markers used with the cell types being investigated, wherever possible, we have used well-categorised antibodies (e.g. PNL2 is an accepted LAM cell marker, not expressed in normal lung [29]) and performed colocalisation studies between LAM cell and stromal cell markers. Whilst HMB-45 is commonly used for diagnosis of LAM, PNL2 is more effective at identifying LAM cells [9,10]. Complementary methodologies support our findings: Ando *et al* isolated single LAM cells by flow cytometry to show that melanoma antigens are associated with both *TSC2* loss of heterozygosity and protein markers of LAM cells [6]. Moreover LAM cells isolated from lymphatic fluids are positive for both melanoma markers and VEGF-D [24]. Using larger cohorts, these associations could be validated in a larger number of cases. It would also be instructive to examine more components of the LAM nodule, such as the hyperplastic type II pneumocytes and inflammatory cells, which are likely to contribute to lung damage, and how they are related to serum markers including VEGF-D.

In summary, we have shown that the composition of LAM nodules evolves during the course of the disease; this is consistent with LAM nodules increasingly comprised of stromal cells expressing CATK with more extensive disease involvement and worsening lung function. Furthermore, CATK is also associated with increased prospective loss of lung function and markers of mTOR complex1 activation are predictive of the benefit of rapamycin therapy. Collectively these findings explain clinical observations that treatment with mTOR inhibitors may be most effective early in the disease course and introduce the idea that those with more advanced disease may benefit from therapies targeted against stromal cells.

## Acknowledgements

We are grateful to Naomi Johnson for Figure 6 and to the women with LAM, who consented to the use of their data in this work. The NIHR Rare disease Translational Research Consortium, The LAM Foundation, The Nottingham Molecular Pathology Node and LAM Action.

## Author contributions statement

SM curated and analysed the samples. IS analysed the images and performed the statistical analysis. DC, R B-J and ISO analysed the samples. SRJ conceived the study,

obtained the funding, saw the patients and analysed the data. All authors contributed to drafting and revision of the manuscript and approved the final version.

## References

- Henske EP, McCormack FX. Lymphangiomyomatosis – a wolf in sheep’s clothing. *J Clin Invest* 2012; **122**: 3807–3816.
- Seyama K, Mitani K, Kumasaka T, *et al.* Lymphangiomyoma cells and lymphatic endothelial cells: expression of VEGFR-3 in lymphangiomyoma cell clusters. *Am J Pathol* 2010; **176**: 2051–2054.
- Goncharova EA, Goncharov DA, Eszterhas A, *et al.* Tuberin regulates p70 S6 kinase activation and ribosomal protein S6 phosphorylation. A role for the TSC2 tumor suppressor gene in pulmonary lymphangiomyomatosis (LAM). *J Biol Chem* 2002; **277**: 30958–30967.
- Carsillo T, Astrinidis A, Henske EP. Mutations in the tuberous sclerosis complex gene TSC2 are a cause of sporadic pulmonary lymphangiomyomatosis. *Proc Natl Acad Sci U S A* 2000; **97**: 6085–6090.
- Clements D, Dongre A, Krymskaya V, *et al.* Wild type mesenchymal cells contribute to the lung pathology of Lymphangiomyomatosis. *PLoS ONE* 2015; **10**: e0126025.
- Ando K, Fujino N, Mitani K, *et al.* Isolation of individual cellular components from lung tissues of patients with lymphangiomyomatosis. *Am J Physiol Lung Cell Mol Physiol* 2016; **310**: L899–L908.
- Liu H-J, Lizotte PH, Du H, *et al.* TSC2-deficient tumors have evidence of T cell exhaustion and respond to anti-PD-1/anti-CTLA-4 immunotherapy. *JCI insight* 2018; **3**: pii: 98674.
- Chilosi M, Pea M, Martignoni G, *et al.* Cathepsin-k expression in pulmonary lymphangiomyomatosis. *Mod Pathol* 2009; **22**: 161–166.
- Martignoni G, Pea M, Reghellin D, *et al.* Molecular pathology of lymphangiomyomatosis and other perivascular epithelioid cell tumors. *Arch Pathol Lab Med* 2010; **134**: 33–40.
- Dongre A, Clements D, Fisher AJ, *et al.* Cathepsin K in lymphangiomyomatosis: LAM cell–fibroblast interactions enhance protease activity by extracellular acidification. *Am J Pathol* 2017; **187**: 1750–1762.
- Johnson SR, Tattersfield AE. Decline in lung function in lymphangiomyomatosis: relation to menopause and progesterone treatment. *Am J Respir Crit Care Med* 1999; **160**: 628–633.
- Gupta N, Lee H-S, Ryu JH, *et al.* The NHLBI LAM registry: prognostic physiologic and radiologic biomarkers emerge from a 15-year prospective longitudinal analysis. *Chest* 2019; **155**: 288–296.
- McCormack FX, Inoue Y, Moss J, *et al.* Efficacy and safety of sirolimus in lymphangiomyomatosis. *N Engl J Med* 2011; **364**: 1595–1606.
- Bee J, Fuller S, Miller S, *et al.* Lung function response and side effects to rapamycin for lymphangiomyomatosis: a prospective national cohort study. *Thorax* 2018; **73**: 369–375.
- Nascimento E, Baldi BG, Mariani AW, *et al.* Immunohistological features related to functional impairment in lymphangiomyomatosis. *Respir Res* 2018; **19**: 83.
- Matsui K, Beasley MB, Nelson WK, *et al.* Prognostic significance of pulmonary lymphangiomyomatosis histologic score. *Am J Surg Pathol* 2001; **25**: 479–484.
- Taveira-DaSilva AM, Hedin C, Stylianou MP, *et al.* Reversible airflow obstruction, proliferation of abnormal smooth muscle cells, and impairment of gas exchange as predictors of outcome in lymphangiomyomatosis. *Am J Respir Crit Care Med* 2001; **164**: 1072–1076.
- Gupta N, Finlay GA, Kotloff RM, *et al.* Lymphangiomyomatosis diagnosis and management: high-resolution chest computed tomography, transbronchial lung biopsy, and pleural disease management. An Official American Thoracic Society/Japanese Respiratory Society Clinical Practice Guideline. *Am J Respir Crit Care Med* 2017; **196**: 1337–1348.
- Miller S, Coveney C, Johnson J, *et al.* The vitamin D binding protein axis modifies disease severity in lymphangiomyomatosis. *Eur Respir J* 2018; **52**: pii: 1800951.
- Corrin B, Liebow AA, Friedman PJ. Pulmonary lymphangiomyomatosis. *Am J Pathol* 1975; **79**: 348–382.
- Hayashi T, Kumasaka T, Mitani K, *et al.* Bronchial involvement in advanced stage lymphangiomyomatosis: histopathologic and molecular analyses. *Hum Pathol* 2016; **50**: 34–42.
- Inoue Y, King TE Jr, Barker E, *et al.* Basic fibroblast growth factor and its receptors in idiopathic pulmonary fibrosis and lymphangiomyomatosis. *Am J Respir Crit Care Med* 2002; **166**: 765–773.
- Pea M, Martignoni G, Bonetti F, *et al.* Tumors characterized by the presence of HMB45-positive perivascular epithelioid cell (PEC) – a novel entity in surgical pathology. *Electron J Pathol Histol* 1997; **3**: 28–40.
- Mitani K, Kumasaka T, Takemura H, *et al.* Cytologic, immunocytochemical and ultrastructural characterization of lymphangiomyomatosis cell clusters in chylous effusions of patients with lymphangiomyomatosis. *Acta Cytol* 2009; **53**: 402–409.
- Paulsson J, Micke P. Prognostic relevance of cancer-associated fibroblasts in human cancer. *Semin Cancer Biol* 2014; **25**: 61–68.
- Kawase A, Ishii G, Nagai K, *et al.* Podoplanin expression by cancer associated fibroblasts predicts poor prognosis of lung adenocarcinoma. *Int J Cancer* 2008; **123**: 1053–1059.
- Psaila B, Lyden D. The metastatic niche: adapting the foreign soil. *Nat Rev Cancer* 2009; **9**: 285–293.
- Chang W, Cane JL, Blakey J, *et al.* Clinical utility of diagnostic guidelines and putative biomarkers in lymphangiomyomatosis. *Respir Res* 2012; **13**: 34.
- Zhe X, Schuger L. Combined smooth muscle and melanocytic differentiation in lymphangiomyomatosis. *J Histochem Cytochem* 2004; **52**: 1537–1542.
- Gulavita P, CDM F, Hirsch MS. PNL2: an adjunctive biomarker for renal angiomyolipomas and perivascular epithelioid cell tumours. *Histopathology* 2018; **72**: 441–448.
- Ruifrok AC, Johnston DA. Quantification of histochemical staining by color deconvolution. *Anal Quant Cytol Histol* 2001; **23**: 291–299.

References 30 and 31 are cited only in the supplementary material.

**SUPPLEMENTARY MATERIAL ONLINE**

**Figure S1.** Example of quantification verification

**Figure S2.** Association of fibroblast surface protein (FSP) with the presence of angiomyolipoma

**Table S1.** Antibodies and antigen retrieval conditions

**Table S2.** Marker reactivity across tissue samples

**Table S3.** Median coefficient of variation in lowest and highest LAM histology score

**Table S4.** Median coefficient of variation by sample type

**Table S5.** Median nodule marker reactivity in lung function tertiles

**Table S6.** Marker reactivity according to phenotype

**Table S7.** Association of nodule marker reactivity with prospective loss of lung function

**Table S8.** Marker reactivity according to rapamycin response